STRUCTURE OF THE STATIC PRESSURE FIELD ON THE ENTRANCE LENGTH OF A PIPE WITH A SHARP INLET EDGE

V. M. Legkii and V. A. Rogachev

UDC 532.57

The three-dimensional static pressure field on the entrance length of a circular pipe with a sharp inlet edge is measured. The field structure, which is characterized by its nonuniformity in the longitudinal and radial directions, is in fairly good agreement with the previously proposed separated flow model and indicates the existence of M-shaped velocity profiles in cross sections of the entrance length.

Pressure tap measurements of the longitudinal surface static-pressure distributions on entrance lengths are widely used as a source of information on flow behavior [1, 2]. However, since only fragmentary characteristics of the state of the pressure field in the wall zone are obtained, the $p_w = f(x/d; Re_d)$ graphs by no means always reflect the three-dimensional structure of the field as a whole in sufficient detail. This makes it necessary to treat with caution conclusions concerning the flow mechanism based on an analysis of the wall static pressure distributions, in particular when the hydrodynamic situation on the entrance length is complicated by separation effects. Below, we discuss the results of investigating the static pressure field on the entrance length of a pipe with a sharp inlet edge for the purpose of gaining a deeper understanding of the qualitative details and exploring the specific points of comparison with the separated flow model proposed in [3].

The diagram in Fig. 1 illustrates the setup of the initial measuring section and the static-pressure probe. In the walls of the measuring section 1, 100-mm long and 36 mm in diameter, we drilled 23 taps 3, each 0.5 mm in diameter. Fifteen of these next to the inlet section had a pitch of 3 mm and the other eight a pitch of 6 mm. The probe 2 consisted of a tip 4, 0.75 mm in diameter, with a hemispherical closed end and two holes 0.08 mm in diameter in the side, together with a hollow holder 5 composed of tubes with a diameter that increased progressively to 2.5 mm. The relative dimensions of the end of the probe tip followed the recommendations made in [4]. The probe was connected by a bracket 6 to a traverse

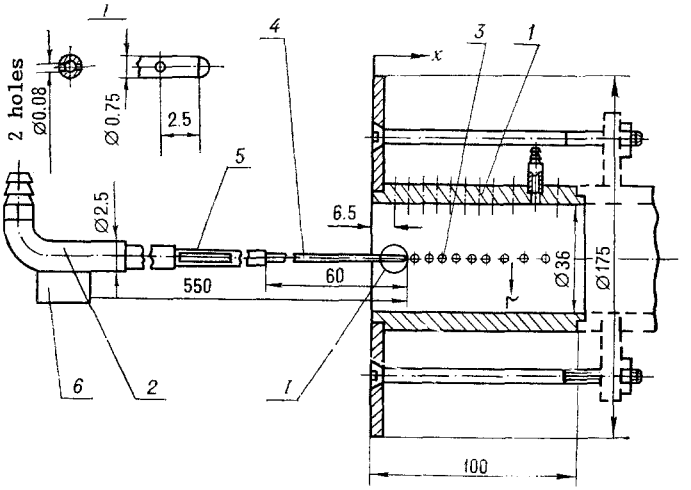

Fig. 1. Entrance measuring section and static-pressure probe: 1) measuring section; 2) static-pressure probe; 3) taps; 4) probe tip; 5) probe holder; 6) probe bracket.

Kiev Polytechnic Institute. Translated from Inzhenerno-fizicheskii Zhurnal, Vol. 61, No. 5, pp. 709-713, November, 1991. Original article submitted March 5, 1991.

0022-0841/91/6105-1311$12.50

mechanism with two degrees of freedom which made it possible to determine the dispalcements correct to ±0.2 mm. For recording the pressure we used MMN-type standard micromanometers. The assembly of the test rig is described in [5].

The static pressure field was investigated under isothermal conditions at Reynolds numbers equal to $13 \cdot 10^3$, $28 \cdot 10^3$, $43 \cdot 10^3$ and $108 \cdot 10^3$ in three series of experiments. In the first series we used the probe to make measurements along the central axis of the entrance length, including the zone preceding the inlet section. In the second series we found the static pressure distributions at the outer edges of the field by means of the taps and the probe, with its axis 0.5 mm from the wall. In the third series we investigated, with the probe, the radial static pressure distributions in a number of discrete cross sections of the entrance length up to x/d = 2.5. In each of these sections the axes of the lateral holes in the probe coincided with the longitudinal coordinate of one of the taps in the wall.

In the first and second series the dimensionless pressure coefficients were calculated from the difference between the local pressure in the flow and the barometric pressure, and in the third series from the difference between the local pressures in the flow and at the wall:

$$C_p^1 = \frac{2(p_i - B)}{\rho w^2}; \quad C_p^2 = \frac{2(p_i - p_{ст})}{\rho w^2}. \tag{1}$$

The $C_p{}^1 = f(x/d; Re_d)$ curves for the axial measurements are plotted in Fig. 2a. When x/d > 0 they are stratified according to the Reynolds number and have a quite sharp minimum in the zone x/d = 0.4-0.42, due to flow contraction. Pressure recovery along the axis continues up to x/d = 1.8-2.0. On the left side of Fig. 2a and to a more convenient scale in Fig. 2b we have shown the experimental data for the interval x/d < 0, which make it possible to estimate the coordinate of the beginning of flow along the pipe axis, if it is associated with the condition $C_p{}^1 = 0$. At Reynolds numbers of the order of 10^5 the coordinate of this point is equal to about three pipe diameters and on the range investigated satisfies the relation $(x/d)_0 \approx 0.045\ Re_d{}^{0.55}$. This relation, which in practice is useful in itself, makes possible a technically sound choice of probe length such as to ensure that the probe is attached far enough in front of the inlet section to exclude deformation of the static pressure field.

The longitudinal static pressure distributions at the outer edges of the field are shown in Fig. 3. The probe and tap measurements are in satisfactory agreement and indicate that the $C_p{}^1 = f(x/d; Re_d)$ graphs obtained in the wall zone and on the axis are essentially nonidentical. Stratified, as on the axis, with respect to the Reynolds number, the curves in Fig. 3 have a fairly extensive zone with a minimum static pressure level on the interval x/d = 0.1-0.35, the absolute value of the pressure coefficient at the walls in the minimum

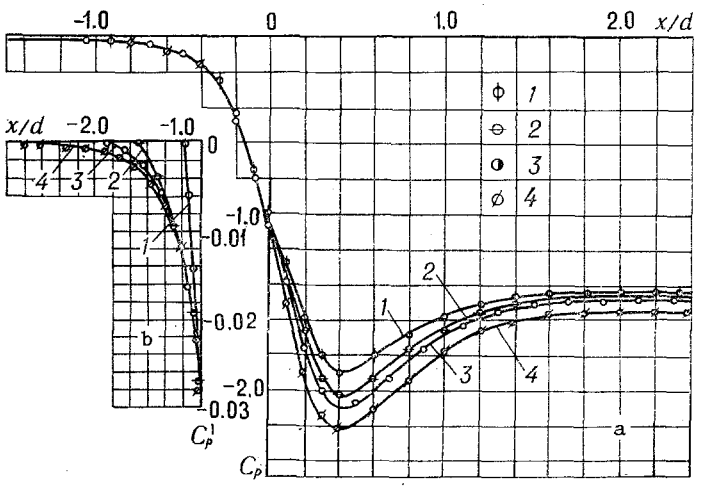

Fig. 2. Results of axial measurements of the static pressure field: a) on the entrance length; b) ahead of the pipe inlet section: 1) $Re_d = 13 \cdot 10^3$; 2) $28 \cdot 10^3$; 3) $43 \cdot 10^3$; 4) $108 \cdot 10^3$.

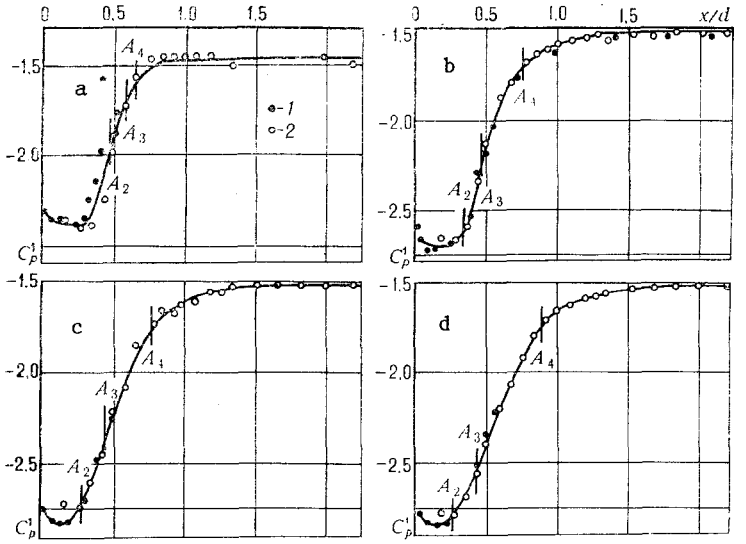

Fig. 3. Results of measuring the static pressure field in the wall zone on the entrance length: 1) probe measurements, 2) tap measurements. a) $Re_d = 13 \cdot 10^3$; b) $28 \cdot 10^3$; c) $43 \cdot 10^3$; d) $108 \cdot 10^3$.

zone being 25-30% lower than on the axis. On the periphery of the field the pressure recovery is much stronger than in the flow core. Thus, when $Re_d = 13 \cdot 10^3$ it ends in the section $x/d = 0.75$, and when $Re_d = 108 \cdot 10^3$ in the section $x/d = 1.7$. In accordance with the data of visualization experiments [3], on the graphs (see Fig. 3) we have indicated the position of the characteristic sections associated with the development of separated flow behind a sharp edge: A_2) the right edge of the hydrometer, A_3) the onset of secondary flow in the boundary layer, and A_4) the section with zero velocity at the wall. As may be seen from the figures, in the configuration of the $C_p^1 = f(x/d; Re_d)$ curves it is not possible to distinguish any features that would permit the identification of the coordinates of these sections or arrival at a physically convincing conclusion with regard to the flow mechanism.

The results of measuring the static pressure field in the radial direction in ten cross sections on the entrance length are shown in Fig. 4. On the range of Reynolds numbers investigated the $C_p^2 = f(x/d; Re_d)$ graphs for different Re_d merge. Characterized by their considerable nonuniformity, especially on the interval $x/d < 0.85$, the radial distributions have a clearly expressed minimum which is gradually displaced towards the flow core as x/d increases. In the immediate proximity of the inlet section the radial coordinate of the pressure minimum is $r/d = 0.43$-0.45, and at a distance $x/d \approx 1.0$ the value is $r/d = 0.37$-0.39. The signs of existence of a pressure minimum disappear when the reduced length reaches $x/d \approx 2.5$. On the $C_p^2 = f(x/d; Re_d)$ graphs, in accordance with the data of [3], we have drawn bars that represent the trajectory of the separated boundary layer.* Despite the tendency for the bars to drift relative to the pressure minimum in the direction of the pipe axis, in all the sections considered their coordinates are closely correlated with the coordinates of the static-pressure minimum. This makes it possible to regard the pressure minimum as the natural consequence of a local and fairly sharp increase in velocity. This reasoning is convincingly confirmed by the experimental data of [6], in which the radial velocity and static pressure distributions in a circular pipe with a sharp inlet edge were measured in parallel in the section $x/d = 0.4$.† Thus, there is reason to believe that in cases of separated flow behind bluff inlet edges on the entrance length of pipes and channels so-called M-shaped velocity profiles are formed in the outer part of the boundary layer.

A theoretical estimate of the error of the probe experiments shows that, as when ordinary pneumometric static-pressure tubes are used, in the middle of the investigated range of the

*The bars correspond to the results of flow visualization at $Re_d = 98 \cdot 10^3$.
†In [6] the inlet to the entrance length of the pipe had no end flange.

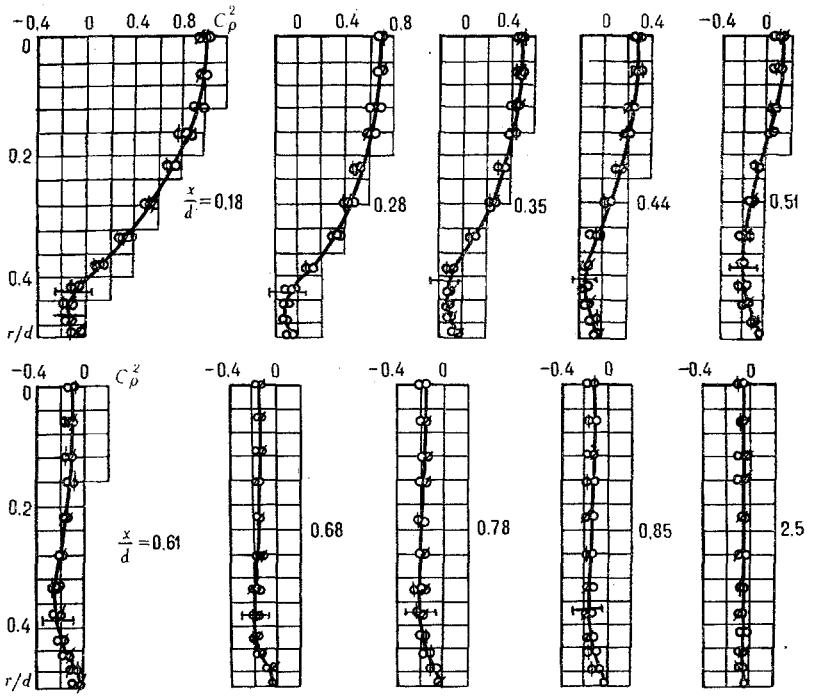

Fig. 4. Results of measuring the radial static pressure distributions on the entrance length; $Re_d = (13–108)\cdot10^3$. For notation see Fig. 2.

Reynolds numbers the probable errors reach 15-25% for a scatter of the experimental data (see Figs. 2-4) which, as a rule, lies within ±10%. The highest of these error values relate to the radial measurements.

Summarizing the results of the investigation, we note the following:

1. The three-dimensional static-pressure field on the entrance length of a pipe with a sharp inlet edge corresponding to the intervals $x/d \leq 2.5$ and $Re_d = (13–108) \times 10^3$ is distinguished by considerable nonuniformity in both the longitudinal and radial directions.

2. Qualitatively, the structure of the static pressure field is consistent with the model proposed in [3], although the experimental data on the state of the field as a whole are not sufficiently informative for the flow mechanism to be discovered.

3. The configuration of the radial static-pressure distributions at $x/d < 2.5$ points to the existence of M-shaped velocity profiles in the outer part of the boundary layer, which is an obvious consequence of separation behind a sharp edge.

NOTATION

x is the longitudinal coordinate, mm; r is the radial coordinate, mm; d is the channel diameter, mm; p is the static pressure, Pa; B is the barometric pressure, Pa; w is the average flow velocity, m/sec; ρ is the density of the air, kg/m^3; Re_d is the Reynolds number calculated from the average flow velocity; and C_p is the static pressure coefficient. Indices: 0 corresponds to the axial coordinate of the point at which $C_p^1 = 0$; 1 corresponds to the measurements on the axis and at the wall; 2 corresponds to the measurements in the radial direction; i denotes the variable coordinate; and w the wall.

LITERATURE CITED

1. D. D. Langren and E. M. Sparrow, J. Basic Engineering, Trans. ASME, Ser. D, 89, No. 1, 233-235 (1967).
2. Ito, Watanabe, Isimaru, and Abe, J. Basic Eng., Trans. ASME, Ser. D, 103, No. 1 (1981).
3. V. M. Legkii and V. A. Rogachev, Inz.-fiz. Zh., 56, No. 2, 215-220 (1989).
4. A. N. Petunin, Gas Flow Parameter Measuring Methods and Techniques [in Russian], Moscow (1972).
5. V. M. Legkii and V. D. Burlei, Teploénergetika, No. 9, 86-88 (1976).
6. I. E. Idel'chik, Prom. Aérodinamika, No. 2, 27-57 (1944).